agriculture

MDPI

Article

Design and Testing of Friction-Type Nail-Tooth-Chain-Plate Residual-Film-Picking System

Deli Jiang [1], Xuegeng Chen [1,*], Limin Yan [1,2], Jinhao Zhang [1], Tao Wu [1] and Xuanhe Fu [1]

[1] College of Mechanical and Electrical Engineering, Shihezi University, Shihezi 832000, China; jiangdeli@stu.shzu.edu.cn (D.J.); yanlm@shzu.edu.cn (L.Y.); zhangjinhao@stu.shzu.edu.cn (J.Z.); wutao@stu.shzu.edu.cn (T.W.); fuxuanhe@stu.shzu.edu.cn (X.F.)

[2] Key Laboratory of Northwest Agricultural Equipment, Ministry of Agriculture and Rural Affairs, Shihezi 832000, China

* Correspondence: 1000005204@ujs.edu.cn; Tel.: +86-139-997-38700

Abstract: Compared with the conventional horizontal conveyor-chain-type plastic-film-picking device, the longitudinal nail-tooth-chain-plate-type plastic-film-picking device developed by our team in the early stage has little tearing effect on the mulching film, and the separation effect of the plastic film and the impurity is better. With a view to further enhancing the performance of the plastic-film-picking device, this study optimized it and designed a friction-type nail-tooth-chain-plate plastic-film-picking chain that does not overload or slip and also facilitates the installation of functional components. The kinematic analysis of the picking nail teeth on the film-picking chain was carried out, and the motion equation and trajectory of the nail teeth during the operation were determined, as well as the requirements for the nail teeth to complete the mulching-film pickup. The key parameters of the plastic-film-picking system were determined by analyzing the no-leakage condition of the plastic film and the force. Moreover, the structural design and key parameters of the shovel-type film-lifting device were determined. According to the design results, a prototype was developed, and a multi-factor test of the operating parameters was carried out. The operating speed, spacing of the pickup nail teeth, depth of the film shovel into the soil, and distance between the tip of the film shovel and center of the picking drum were used as the experimental factors. The plastic-film pickup rate, impurity rate of the recovered mulching film, and traction resistance were used as the test indicators. A four-factor, five-level quadratic regression orthogonal combination experiment was conducted using the Central Composite Design (CCD). The effect of each test factor on the test index of the plastic-film-picking system was studied, the regression models were established, and the optimal parameter combination was acquired by using the multi-objective optimization method. When the working speed was 6 km/h, the pickup-nail-tooth spacing was 228.6 mm, the depth of the film-lifting shovel into the soil was 37 mm, and the distance between the tip of the film shovel and the center of the pickup drum was 130 mm, the field experiment shows that the plastic-film pickup rate was 90.12%, the impurity rate of the recovered mulching film was 8.96%, and the traction resistance was 19.905 kN. The relative errors between the test results and the predicted values of the regression models were less than 5%, indicating that the parameter optimization regression models were reliable, and the designed friction-type nail-tooth-chain-plate plastic-film-picking system met the technical requirements of agricultural-plastic-film recycling. The research results can provide a technical reference for the development of mulching-film collection machines.

Keywords: agricultural machinery; design; test; residual-film recovery; friction-type nail-tooth chain; film-lifting device

Citation: Jiang, D.; Chen, X.; Yan, L.; Zhang, J.; Wu, T.; Fu, X. Design and Testing of Friction-Type Nail-Tooth-Chain-Plate Residual-Film-Picking System. *Agriculture* **2024**, *14*, 512. https://doi.org/10.3390/agriculture14040512

Received: 25 January 2024
Revised: 12 March 2024
Accepted: 19 March 2024
Published: 22 March 2024

1. Introduction

Plastic-film-mulching cultivation technology has the advantages of heat preservation, moisture conservation, the inhibition of weed growth, improvement in the soil aggregate structure, and increases in crop yields, and it has made a significant contribution to the increase in agricultural production and efficiency in China [1,2]. Xinjiang contains China's main high-quality cotton-producing areas, almost all of which use plastic-film-mulching planting technology [3,4]. The annual cotton plastic-film-mulching planting area in Xinjiang is nearly 2.5 million hm^2, and the use of agricultural plastic film is more than 180,000 tons [5]. However, due to the failure to effectively recycle the plastic film after use, the mulching film in the soil has increased year by year, causing serious plastic pollution [6,7]. Farmland-residual-film mechanical recycling is able to cover a large area, is highly efficient in agricultural-plastic-film recovery, and has become an effectual measure to solve plastic-film pollution [3]. Numerous scientific researchers have developed various mulching-film collection machines after years of effort [8–11]. Xinjiang's cotton-field residual-film-recycling machinery is mainly large machinery, mostly compound combined-operation machinery, including folding-vertical-rod film machines and straw-crushing and residual-film-collection combined-operation machinery, and it has been applied in production, achieved good recovery effects, to a certain extent, and improved the Xinjiang cotton-field residual-film pollution problem.

Plastic-film picking is an important part of mechanized plastic-film recovery. It is required to pick up the plastic film smoothly during the operation and effectively connect it with the subsequent operation. The structure form and operation quality of the pickup device play a key role in the recovery effect of agricultural plastic film. According to the picking principle, the plastic-film-picking mechanism can be divided into the telescopic-tooth-rod-roller type, elastic-tooth type, lever type, gear-tooth type, conveyor-chain type, and so on [12–15]. The main body of the conveyor-chain-type plastic-film-picking mechanism is the conveyor chain, supplemented by the pickup teeth composed of tooth rods, scrapers, or conveyor belts. When the conveyor chain rotates, the film pickup teeth pick up the film and move it along the conveyor chain to complete the spatial transfer of the film, so as to achieve the purposes of picking up and transporting the mulching film. The plastic-film pickup mechanism with the conveyor chain has a high collection rate for mulching film, and it can separate the film from impurities in the process of plastic-film pickup and transportation, reduce the impurity content in the recovered plastic film, and provide preconditions for the resource utilization of the residual film. For example, the residual-film-recovery rate of the finger-chain residual-film-recycling machine designed by Kou et al. [16] was 92.85%, and the residual-film-impurity rate was 26.05%. The rake-type surface-residual-film-recycling machine with a guide chain designed by Cao and Xie et al. [17,18] has a residual-film-recovery rate of more than 88% and a residual-film-impurity rate of 12%. The vertical-double-row-chain residual-film-recycling machine designed by Shi et al. [19] has a residual-film pickup rate of 86.7% and an impurity rate of 35.9% under the optimal parameter combination.

In the early stage, a cotton-field residual-film-recovery machine was designed. Different from the conventional horizontal conveyor-chain plastic-film-picking device, the film-picking mechanism is a longitudinal plastic-film-picking chain, which is composed of a special nail-tooth-chain-plate unit [20]. The field test results of the physical prototype show that the residual-film-picking rate is more than 90%, and the impurity rate is less than 10% [20,21]. In addition, the longitudinal plastic-film-picking chain is flexible and has little tearing effect on the plastic film. It can realize the whole film-picking process, promote the effective separation of the agricultural plastic film and impurities, and reduce the impurity content of the recovered film. However, the pickup chain plate has significant wear, and the pickup device, driven by pins, cannot achieve overload protection.

In response to these problems, a friction-type nail-tooth-chain-plate plastic-film-picking chain that not only does not overload and skid but also facilitates the installation of functional components was optimized and designed, and the film-lifting components were improved to assist the plastic-film pickup. By analyzing the functional and structural requirements of the friction-type plastic-film-picking chain, some structural parameters were determined. The working mechanism, movement, and residual-film force of the plastic-film-picking chain were analyzed to determine the conditions for realizing residual-film picking, no-leakage picking, and conveyance. By making a physical prototype and conducting field experiments, Design-Expert 13 software was used to explore the influence of the key factors of the residual-film-picking system on the experimental indexes, such as the residual-film-picking rate, residual-film-impurity rate, and traction resistance, by using the four-factor and five-level quadratic regression orthogonal combination test. The quadratic regression model was used to optimize the best working parameters of the friction-type nail-tooth-chain-plate residual-film-picking system, and the experimental verification was carried out. The research can provide a basis for further optimizing the equipment of residual-film-recycling machines in Xinjiang cotton fields.

2. Structure and Working Principle

2.1. The Whole Machine Structure and Working Principle

Plastic-film mulching is commonly used for cotton cultivation in Xinjiang. In order to adapt to the development of the full mechanization of cotton, a wide and narrow row spacing of 100 mm + 660 mm is planted according to the machine-picked cotton mode, with a film width of 2050 mm and six rows of cotton [22,23]. According to the cotton-planting mode, the structure and operation process of the machine for returning straw to the field and residual-film recycling are shown in Figure 1. The combined-operation machine is mainly composed of a traction device, straw-crushing device, plastic-film-picking-and-conveying device, film-lifting device, impurity-conveying device, and film-rolling device.

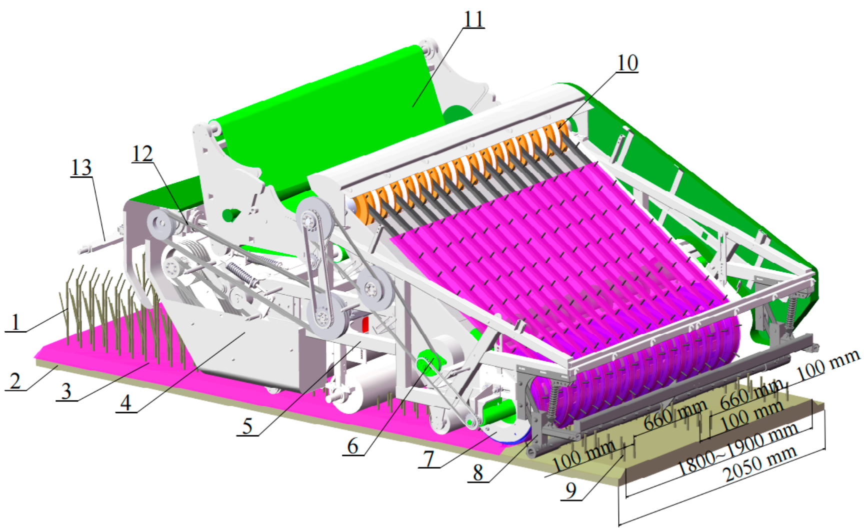

Figure 1. The structure and working process of the combined straw-crushing and residual-film-recycling machine. 1. Cotton stalks; 2. soil; 3. mulching film; 4. straw-crushing device; 5. frame; 6. impurity-conveying device; 7. plastic-film-picking-and-conveying device; 8. mulching-film-lifting device; 9. cotton stalk stubble; 10. plastic-film-stripping device; 11. plastic-film-rolling device; 12. transmission system; 13. traction device.

When the combined straw-crushing and residual-film-recovery machine is working, the tractor pulls the machine forward, and the output power is transmitted to each component through the universal-joint transmission shaft and transmission system. The combined machine picks up one piece of plastic film at a time with a width of 2050 mm. With the advance of the machine, the straw-crushing device crushes the cotton stalks, and the crushed cotton stalks are transported to the right side of the forward direction of the machine through the screw conveyor. Then, the film-lifting device separates the film from the soil, and the film-picking-and-conveying device picks up the separated residual film, flips it 180°, and transports it upward. In the process of plastic-film conveyance, the impurities on the upper surface of the plastic film are separated from the residual film under the actions of gravity and vibration, fall into the impurity-conveying device, and are transported to the outside of the machine. When the residual film moves to the stripping device and falls into the film-rolling device, it is packaged into a roll with the movement of the film-rolling device. The hydraulic device is started to unload the film and complete the residual-film-recovery operation.

2.2. Structure and Working Principle of Friction-Type Nail-Tooth-Chain-Plate Residual-Film-Picking System

The residual-film-picking system is composed of a film-lifting device, friction-type plastic-film-picking chain, connecting side plate, picking rotary drum, and film-stripping device, as shown in Figure 2. The picking rotary drum, friction-type plastic-film-picking chain, and film-stripping device form a chain drive and are connected to the combined machine frame through the bearing seat, which can rotate around the central axis of the film-stripping device to realize the profiling. A plurality of pickup nail teeth are installed on the pickup chain, and several pickup chains are arranged at a certain distance. The film-lifting device is fixed with the frame of the combined working machine and is located at the end of the machine. The front end of the film-lifting device is designed with a film shovel, and the film-lifting shovel and film-picking chain are staggered. Different from the conventional design of the film-collecting process, the residual-film-picking system developed in this paper is a flexible, multi-group, longitudinal film-picking chain, which can reduce the tearing of the film by the film-picking mechanism and realize the whole film-picking process. Furthermore, the residual film is turned 180° during the picking process so that the impurities on the surface of the film are downward, which is more conducive to the separation of the plastic film and impurities and reduces the impurity content of the recovered residual film.

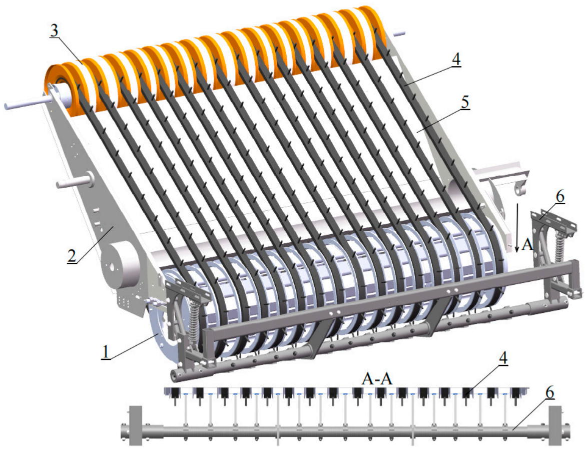

Figure 2. Structure of residual-film-picking system. 1. Picking rotary drum; 2. connecting side plate; 3. plastic-film-stripping device; 4. friction-type plastic-film-picking chain; 5. impurity guide plate; 6. mulching-film-lifting device.

The working principle of the friction-type nail-tooth-chain-plate residual-film-picking system is shown in Figure 3. The film-lifting device is buried at a certain depth under the action of the depth-limiting-spring pressure. As the combined machine moves forward, the film shovel loosens the soil under the mulching film to separate the film from the soil. The residual film is attached to the surface of the film shovel. Under the action of the gravity of the pickup system, the pickup nail teeth are buried into the soil to break the residual film, and the film is picked up and flipped 180° with the movement of the pickup chain. As the picking chain continues to move, the impurities on the upper surface of the mulching film fall into the picking rotary drum or the impurity guide plate. When the plastic film moves to the film-stripping device, it comes into contact with the outer circle of the stripping ring. Due to the height difference between the picking nail tooth and the outer circle of the stripping ring, the plastic film is pulled. Under tensile force, the plastic film moves to the end of the picking nail tooth to complete the stripping, and then the residual film falls into the film-rolling device.

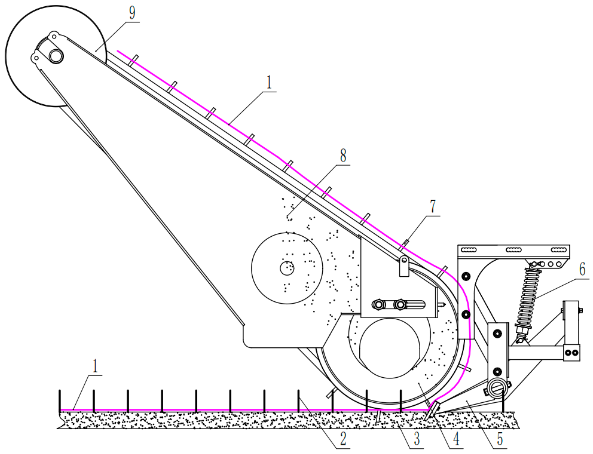

Figure 3. Working-principle diagram of residual-film-picking system. 1. Mulching film; 2. cotton stalk stubble; 3. soil; 4. picking rotary drum; 5. film-lifting shovel; 6. depth-limiting spring; 7. pickup nail teeth; 8. impurity; 9. plastic-film-stripping device.

3. Design and Analysis of Key Components

3.1. Design of Friction-Type Plastic-Film-Picking Chain

The pre-designed plastic-film-picking chain is shown in Figure 4a, which has a steel-chain-plate structure. To tackle the problem that the picking-chain plate driven by pins has significant wear and cannot achieve overload protection, this study optimized and designed a friction-type plastic-film-picking chain that not only does not overload or slip during the transmission process but also facilitates the installation of functional components. It is mainly composed of a rubber-chain friction block connecting the chain plate, pin shaft, and pickup nail tooth, as shown in Figure 4b.

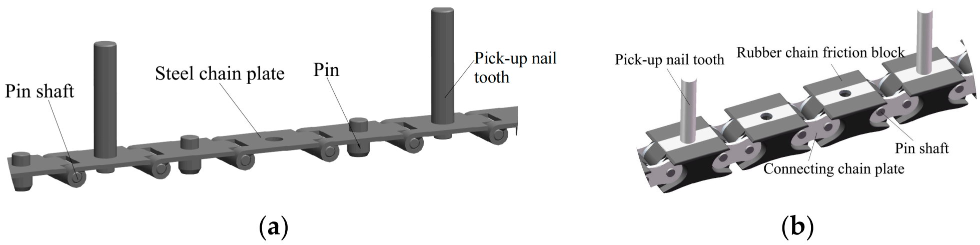

Figure 4. Plastic-film-picking chain structure. (**a**) Steel chain plate; (**b**) friction-type chain plate.

The rubber-chain friction block is hinged with the connecting chain plate through the pin shaft. Multiple sets of rubber-chain friction blocks and connecting chain plates are connected end to end to form a closed friction chain. There is a hole on the rubber-chain friction block to install the pickup nail teeth. The friction pin-tooth chain relies on the side of the rubber-chain friction block to contact the V-shaped drive wheel to generate friction to transmit motion and power. A single friction-type plastic-film-picking chain, a driving wheel, and a chain-plate guide rail form the chain transmission system, as shown in Figure 5.

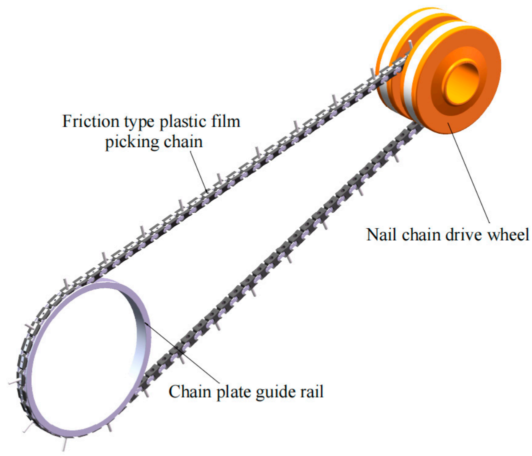

Figure 5. Chain drive system.

3.1.1. Rubber-Chain Friction Block

The rubber-chain friction block is mainly composed of a rubber body, a metal-chain-plate skeleton, and a shaft sleeve. The structure is shown in Figure 6a. The shaft sleeve is pressed and riveted in two through holes of the metal-chain-plate skeleton, and then the rubber body, the metal-chain-plate skeleton, and the shaft sleeve form a rubber-chain friction block through the rubber vulcanization process. O_1 and O_2 are circular reference holes, which play the role of positioning the hinge position. The main design parameters of the rubber-chain friction block include the basic pitch (P), the inner radius of the sleeve (r_0), the outer radius of the sleeve (r_1), the radius of the rubber body (r_2), the radius of the metal-chain-plate skeleton (r_3), the bottom radius of the rubber body (r), the wedge angle (α), the top width (b), the height (h_0), etc., as shown in Figure 6b.

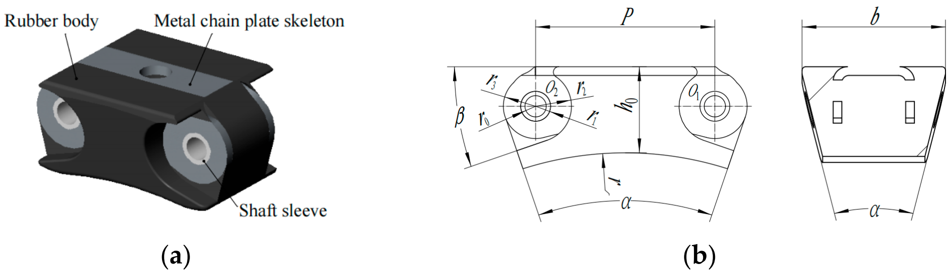

Figure 6. Structure and parameter diagram of rubber-chain friction block: (**a**) structure; (**b**) parameters.

The designed rubber-chain friction block can be matched with the standard single-row-roller-chain inner chain plate. The larger the pitch (P), the higher the bearing capacity, but the overall size increases, the polygon effect is significant, and the vibration, impact, and noise are more serious [24,25]. However, when the center distance is large and the transmission ratio is small, a large-pitch chain drive should be selected. Combining the bearing capacity of the chain plate and the pickup-nail-teeth spacing, the 12A inner chain plate was selected as the connecting chain plate, and the pitch is 19.05 mm. In order to increase the friction area of the rubber-chain friction block and install the fixed pickup nail teeth at the same time, the rubber-chain friction block was designed according to the size of the E-type V belt [26]. The top width (b) is 39 mm, the height (h_0) is 24 mm, and the wedge angle (α) is 29°. The pitch (P) of the rubber-chain friction block (P) is 2 times that of the connecting chain plate, which is 38.1 mm. The inner radius (r_0) of the sleeve is matched with the pin shaft of 12A. The rubber-body radius (r_2) and metal-chain-plate skeleton radius (r_3) matched with the inner-chain-plate width are 10 m and 9 mm, respectively. The bottom radius (r) of the rubber body is 94 mm.

3.1.2. Pickup Nail Teeth

The length of pickup nail tooth determines the effect of the mulching-film picking. If the nail tooth is too short, the film easily falls off, and if it is too long, the power consumption of the machine is increased, and this is not conducive to the falling off of the plastic film. The main design parameters of the pickup nail tooth include the overall length (l_0), the maximum depth of the nail tooth into the soil (L), and the diameter (d), as shown in Figure 7.

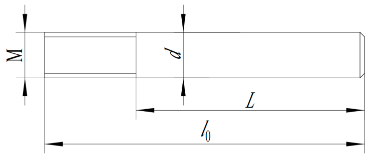

Figure 7. Pickup-nail-tooth parameter diagram.

The bottom end of the pickup nail tooth is designed with a thread, which is connected with the metal-chain-plate skeleton through the nut, so as to facilitate the replacement of the nail tooth after wear or bending deformation during the film-recycling operation. Based on previous research [20], the diameter of the nail tooth (d) is 10 mm, the thread diameter is M10, and the maximum depth of the nail tooth into the soil (L) is 50 mm. According to the thickness of the rubber-chain friction block, the overall length of the pickup nail tooth (l_0) is 70 mm.

3.1.3. Drive Wheel of Nail-Toothed Chain

According to the structure of the rubber-chain friction block, the drive wheel of the nail-toothed chain is determined, which is mainly composed of two film-stripping rings in opposite directions, as shown in Figure 8. The film-stripping ring is formed by pressing the steel plate, and the two opposite stripping rings are separated by a certain distance. The convex slope forms a V shape, which is matched with the rubber-chain friction block. The main design parameters of the nail-toothed-chain drive wheel include the radius (R_1) in contact with the bottom surface of the rubber-chain friction block, the spacing (b_d) between the two film-stripping rings, the groove angle (φ), the outer diameter (d_a) of the inclined plane, and the outer diameter (D) of the film-stripping ring. The spacer rings are welded on the outer sides of the film-stripping rings. One plays a supporting role, and the other realizes the arrangement of the friction-type nail-tooth chain according to the designed size. The film-stripping rings and spacer rings are welded onto the film-stripping roller at the same time. When the film-stripping roller rotates, it drives the stripping ring to rotate. The wedge angle (α) of the friction block of the rubber chain is 29°, and the groove angle (φ) between the inclined planes of the two film-stripping rings is 28°. The top width (b) of the rubber-chain friction block is 39 mm, and the distance (b_d) between the two stripping rings is 42 mm. R_1 is determined by the rotation ratio between the picking rotary drum and the stripping roller.

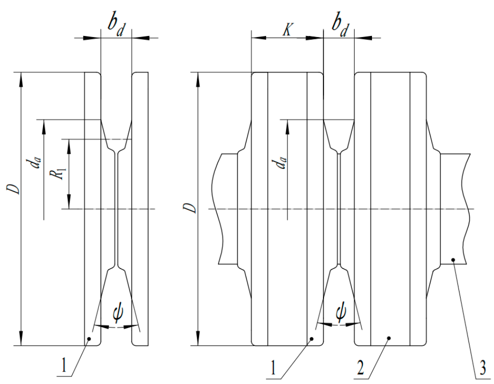

Figure 8. Structure and parameter diagram of nail-chain drive wheel. 1. Plastic-film-stripping ring; 2. spacer ring; 3. plastic-film-stripping roller.

3.2. Kinematic Analysis of Friction-Type Plastic-Film-Picking Chain

The rotary motion of the friction-type plastic-film-picking chain and the forward motion of the machine form a composite motion trajectory. The coordinate system is established with the center (O) of the chain-plate guide rail as the origin. The positive direction of the x-axis is the forward direction of the machine, and the positive direction of the y-axis is vertical upward, as shown in Figure 9.

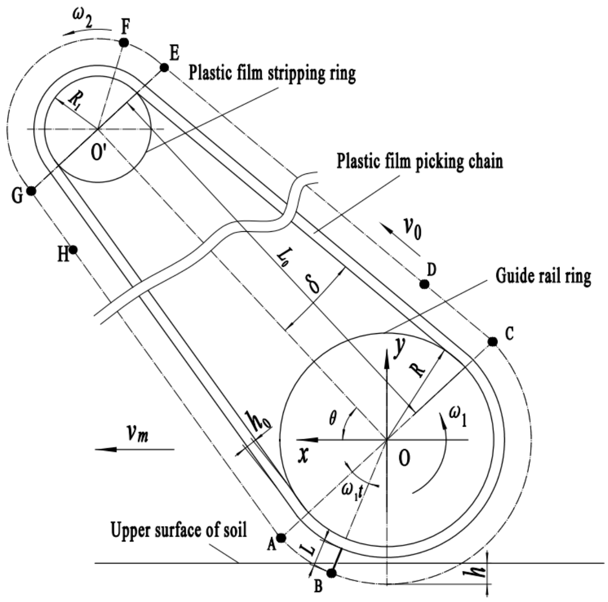

Figure 9. Motion analysis diagram of plastic-film-picking chain.

The working speed of the combined machine is v_m, the rotation speed of the film-stripping roller is ω_2, the picking rotary drum is ω_1, and the depth of the nail teeth into the soil is h. Point A is the intersection point of the linear and rotary motion of the pickup chain. When the machine runs for t s, the motion equations of the end of the nail tooth at each point are obtained:

$$\text{B point}: \begin{cases} x_B = v_m t + (R + h_0 + L)\cos(\frac{\pi}{2} - \theta + \omega_1 t - \delta) \\ y_B = -(R + h_0 + L)\sin(\frac{\pi}{2} - \theta + \omega_1 t - \delta) \end{cases} \tag{1}$$

where R is the radius of the guide-rail ring (m); θ is the inclination angle between the pickup device and the horizontal plane (rad, $\theta = \pi/3$); δ is the angle between the center line of the picking chain and the conveying section of the picking chain (rad).

$$\omega_1 = \frac{v_0}{R + h_0 + L} \tag{2}$$

where v_0 is the plastic-film-pickup-conveying speed (m·s^{-1}).

$$\text{D point}: \begin{cases} x_D = v_m t - (R + h_0 + L)\sin(\theta - \delta) + L_{CD}\cos(\theta - \delta) \\ y_D = (R + h_0 + L)\cos(\theta - \delta) + L_{CD}\sin(\theta - \delta) \end{cases} \tag{3}$$

where L_{CD} is the linear distance from point C to point D (m).

Among them,

$$L_{CD} = v_0(t - t_0) \tag{4}$$

where t_0 is the time of the nail teeth from point A to point C (s).

$$t_0 = \frac{\pi + 2\delta}{\omega_1} \tag{5}$$

$$\text{F point}: \begin{cases} x_{\mathrm{F}} = v_m t - (R_1 + h_0 + L)\cos[\frac{\pi}{2} - \theta + \omega_2(t - t_0 - t_0{}') + \delta] + L_0\cos\theta \\ y_{\mathrm{F}} = L_0\sin\theta + (R_1 + h_0 + L)\sin[\frac{\pi}{2} - \theta + \omega_2(t - t_0 - t_0{}') + \delta] \end{cases} \tag{6}$$

where $t_0{}'$ is the time of picking up the movement of the nail teeth from point C to point E (s).

$$\omega_2 = \frac{v_0}{R_1 + h_0 + L} \tag{7}$$

$$t_0{}' = \frac{L_0}{v_0} \tag{8}$$

where L_0 is the central distance from the guide ring to the plastic-film-stripping ring (m).

$$\text{H point}: \begin{cases} x_{\mathrm{H}} = v_m t + L_0\cos\theta + (R_1 + h_0 + L)\sin(\theta + \delta) - L_{\mathrm{GH}}\cos(\theta + \delta) \\ y_{\mathrm{H}} = L_0\sin\theta - L_{\mathrm{GH}}\sin(\theta + \delta) - (R_1 + h_0 + L)\cos(\theta + \delta) \end{cases} \tag{9}$$

where L_{GH} is the linear distance from point G to point H (m).

$$L_{\mathrm{GH}} = v_0[t - (t_0 + t_0{}' + t_0{}'')] \tag{10}$$

where $t_0{}''$ is the time of picking up the movement of the nail teeth from point E to point G (s).

$$t_0{}'' = \frac{\pi - 2\delta}{\omega_2} \tag{11}$$

The analysis in Figure 9 shows that the nail tooth picks up the film in the ABC arc section, completes the film delivery in the CDE straight section, and completes the film removal in the EFG section. By deriving the displacement equation of the nail teeth at each motion point to time, the motion speed of the pickup nail teeth at each stage can be obtained.

The speed of the nail teeth in the ABC arc section is as follows:

$$\begin{cases} v_{\mathrm{Bx}} = \dot{x}_{\mathrm{B}} = v_m + \omega_1(R + h_0 + L)\sin(\frac{\pi}{2} - \theta + \omega_1 t - \delta) \\ v_{\mathrm{B}y} = \dot{y}_{\mathrm{B}} = -\omega_1(R + h_0 + L)\cos(\frac{\pi}{2} - \theta + \omega_1 t - \delta) \end{cases} \tag{12}$$

The speed of the nail teeth in the CE straight section is as follows:

$$\begin{cases} v_{\mathrm{Dx}} = \dot{x}_{\mathrm{D}} = v_m + v_0\cos(\theta - \delta) \\ v_{\mathrm{Dy}} = \dot{y}_{\mathrm{D}} = v_0\sin(\theta - \delta) \end{cases} \tag{13}$$

The speed of the nail teeth in the EFG arc section is as follows:

$$\begin{cases} v_{\mathrm{F}x} = v_m - \omega_2(R_1 + h_0 + L)\sin[\frac{\pi}{2} - \theta + \omega_2(t - t_0{}' - t_0) + \delta] \\ v_{\mathrm{F}y} = \omega_2(R_1 + h_0 + L)\cos[\frac{\pi}{2} - \theta + \omega_2(t - t_0{}' - t_0) + \delta] \end{cases} \tag{14}$$

The speed of the nail teeth in the GA straight section is as follows:

$$\begin{cases} v_{\mathrm{H}x} = \dot{x}_{\mathrm{H}} = v_m - v_0\cos(\theta + \delta) \\ v_{\mathrm{H}y} = \dot{y}_{\mathrm{H}} = -v_0\sin(\theta + \delta) \end{cases} \tag{15}$$

The ratio of the line speed of the endpoint of the nail tooth (v_0) to the working speed of the machine (v_m) (referred to as the pickup-speed ratio) is λ. Then,

$$\lambda = \frac{v_0}{v_m} \tag{16}$$

In order to verify the correctness of the equations established by the pickup nail teeth at each point, the static trajectory curve of the pickup-nail-tooth endpoint is drawn by MATLAB 2015b, as shown in Figure 10a. The figure shows that when the pickup nail teeth only rotate with the friction-type plastic-film pickup chain without forward movement, the static trajectory curve of the nail-tooth endpoint is consistent with the structure of the pickup device, so the established pickup-nail-tooth endpoint trajectory equation is correct. Taking different values of λ, the dynamic trajectory curve of the endpoint of the pickup nail was drawn by MATLAB 2015b, as reflected in Figure 10b. Moreover, the velocity curve of the nail tooth in a cycle was drawn, as reflected in Figure 10c.

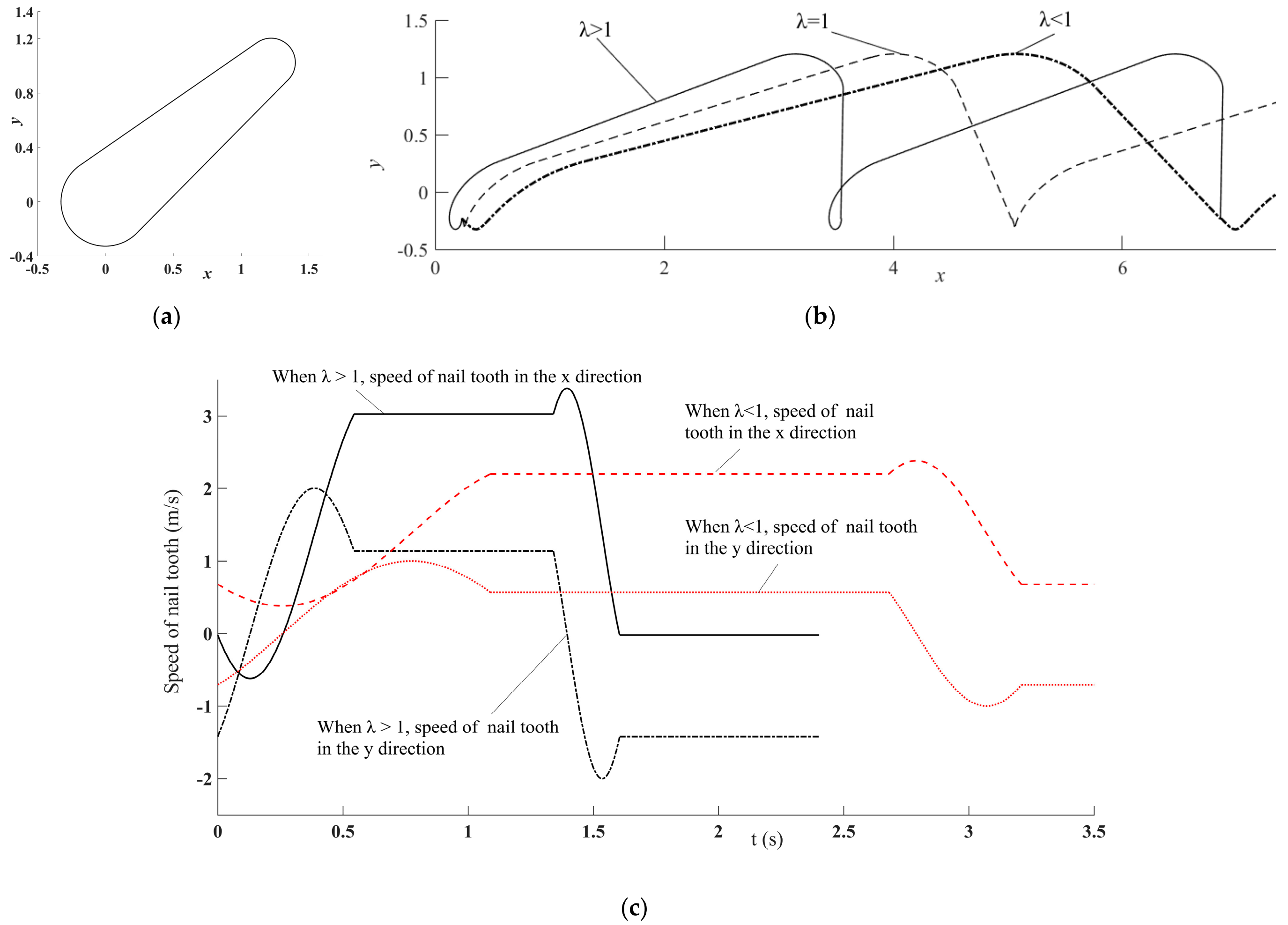

Figure 10. Endpoint trajectory and velocity curve of pickup nail teeth: (**a**) static trajectory curve; (**b**) endpoint motion trajectory of pickup nail teeth under different speed ratios (λ); (**c**) speed curve graph of pickup-nail-tooth endpoint within one cycle.

According to Figure 10b,c, when λ < 1, the speed of the pickup nail tooth in the x direction is greater than 0 when it moves in the ABC arc segment, and it decreases first and then increases. The speed remains unchanged in the CE straight-line segment. In the EFG arc segment, the speed in the x direction increases first and then decreases, and the speed in the GA straight-line segment remains unchanged. At this time, the speed of the nail tooth in the y direction increases first and then decreases in the ABC arc segment, and the speed remains unchanged in the CE straight-line segment. When moving to the EFG arc segment, the speed of the nail tooth in the y direction decreases first and then increases, and then the speed remains unchanged in the GA straight-line segment. When λ > 1, the velocity variation in the nail tooth in the x and y directions is consistent with that when λ < 1, but the velocity value in the y direction is greater than that when λ < 1 because when λ > 1, the increase in the v_0 increases the velocity component on the y-axis. At the same time, when λ > 1, when the pickup nail teeth move in the ABC arc section, the speed in the x direction is less than 0. At this time, the speed of the pickup teeth in the horizontal direction is opposite to the forward speed of the machine, and the pickup teeth have the action of picking up the plastic film backward.

It can be seen from Figure 10b that when $\lambda > 1$, the pickup-nail-tooth movement forms the pickup ring buckle, but when $\lambda \leq 1$, the pickup-nail movement does not form the pickup ring buckle. Therefore, to ensure that the plastic film is collected smoothly, λ should be greater than 1; that is, the residual-film-picking-and-conveying speed (v_0) should be greater than the forward speed (v_m) of the machine. At this time, the rotation distance of the pickup nail teeth is greater than the forward-movement distance of the chain. The plastic film between the two adjacent pickup nail teeth on the same plastic-film-picking chain is in a tensile state. The residual film under tension is tightened between the two nail teeth. The plastic film does not easily wrap impurities, which is conducive to cleaning operations. Simultaneously, under the action of plastic-film elasticity, the pickup nail teeth are pulled by the residual film. The tension is perpendicular to the axis of the nail teeth, which increases the friction between the film and nail teeth, which is beneficial to the film collection.

3.3. Analysis of Mulching-Film No-Missed-Picking Condition

In the friction-type plastic-film-picking chain operation, the nail teeth arranged on the chain pick up the mulching film on the surface in turn. To ensure the mulching film is not missed in the pickup, the latter nail tooth of the adjacent two nail teeth on the same picking chain is required to enter the soil before the former nail tooth leaves the soil [27]. The trajectory of the two adjacent pickup teeth is shown in Figure 11.

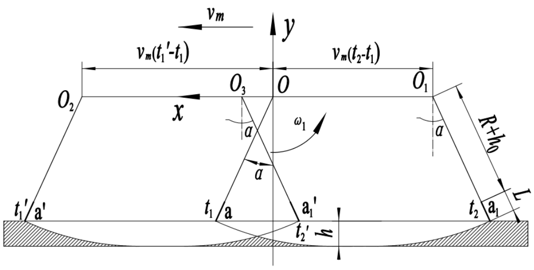

Figure 11. Motion trajectory analysis of two adjacent pickup nail teeth.

From the trajectory equation of picking up the nail tooth and Figure 11, the following can be obtained:

$$\begin{cases} OO_1 = v_m(t_2 - t_1) \\ OO_2 = v_m(t_1{}' - t_1) \\ O_2O_3 = v_m(t_2{}' - t_1{}') \\ OO_3 = OO_2 - O_2O_3 \end{cases} \quad (17)$$

where t_1 is the time that the previous pickup nail teeth enter the soil (s); t_2 is the time when the previous nail tooth is unearthed (s); $t_1{}'$ is the time when the latter pickup nail teeth enter the soil (s); $t_2{}'$ is the time when the latter nail is unearthed (s); OO_1 is the horizontal movement distance of the picking drum from the time of the entry to the excavation of the previous nail tooth (m); OO_2 is the horizontal moving distance of the pickup drum at the time that two adjacent nail teeth enter the soil (m); O_2O_3 is the distance that the pickup cylinder moves horizontally during the time from the entry to the excavation of the latter nail tooth (m); OO_3 is the distance that the pickup drum moves horizontally during the time from the entry of the previous nail tooth to the excavation of the subsequent nail tooth (m).

$$\begin{cases} t_2 - t_1 = t_2{}' - t_1{}' = \frac{2\alpha}{\omega_1} \\ t_1{}' - t_1 = \frac{L_1}{v_0} \end{cases} \quad (18)$$

where α is the angle between the nail teeth and the vertical direction when they are buried in the soil (rad).

The simplified equation can be obtained as follows:

$$OO_3 = \frac{v_m L_1}{v_0} - \frac{2 v_m \alpha}{\omega_1} = \frac{v_m}{v_0}(L_1 - 2\alpha(R + h_0 + L)) \tag{19}$$

When a_1' and a overlap, that is, when the former nail tooth leaves the soil, the latter nail tooth enters the soil, and the critical condition is as follows:

$$OO_3 \leq 2(R + h_0 + L)\sin\alpha \tag{20}$$

Combining Equations (19) and (20), we obtain the following:

$$\frac{L_1 - 2\alpha(R + h_0 + L)}{2\sin\alpha(R + h_0 + L)} \leq \lambda \tag{21}$$

According to Equation (21), when the structure of the device is determined, the residual-film non-leakage pickup is related to the pickup-speed ratio (λ) and the distance between the adjacent pickup nail teeth (L_1). According to the pitch of the rubber-chain friction block (38.1 mm) and the pitch of the connecting chain plate (19.05 mm), the minimum distance between the adjacent nail teeth (L_1) is 57.15 mm; that is, a pickup nail tooth is installed on each rubber-chain friction block. Furthermore, the L_1 can be 114.3 mm, 171.45 mm, and so on when the nail teeth are installed at intervals on the rubber-chain friction block.

3.4. Force Analysis of Residual Film

The friction-type nail-pickup chain can be divided into four processes: the mulching-film-puncturing process, mulching-film-picking process, mulching-film-hanging process, and mulching-film-conveying process, as shown in Figure 12a. Among them, the process from the nail teeth entering the soil (a) to their unearthing (a_1) is the process of puncturing the film. From a_1 to b is the film-picking process, from b to e is the film-hanging process, and from e to e_2 is the film-conveying process. The four processes correspond to four operating areas. The stresses of the plastic film in the four processes were analyzed separately, as shown in Figure 12b.

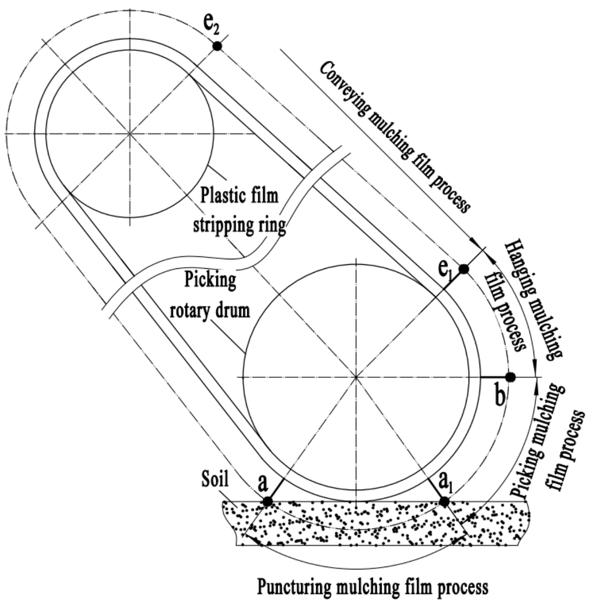

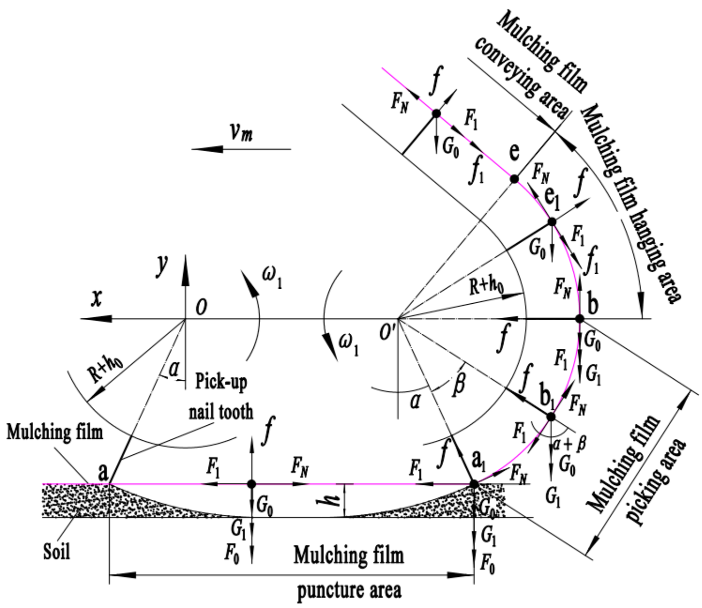

Figure 12. Division of plastic-film-picking process and force analysis: (**a**) partition of plastic-film-picking process; (**b**) force analysis of plastic-film-picking process.

When the mulching film was recovered after autumn, there was soil and a small amount of cotton straw on the film, and there was adhesion between the residual film and the soil. When the friction-type plastic-film-picking chain picks up the plastic film, the direction of the pickup nail teeth is opposite to the direction of the machine operation. The condition for separating the film from the surface is that the pickup nail teeth work on the plastic film to overcome the pressure of the impurities on the surface of the mulching film, the gravity of the film itself, and the adhesion between the mulching film and the soil. In the process of puncturing the film, the film is subjected to its own gravity (G_0), the impurity gravity (G_1) on the film surface, the adhesion force (F_0) between the residual film and the soil, the nail-tooth friction (f), the support force (F_N), and the residual-film elasticity (F_1). Because the running speed of the nail teeth (i.e., the linear speed of the circumferential section of the nail teeth) is higher than the working speed of the machine, the mulching-film-picking process is pulled to form the residual-film elasticity (F_1). In the process of picking up the film, the film is subjected to five forces: the G_0, G_1, f, F_N, and F_1. In the film-hanging process, in addition to the G_0, f, F_N, and F_1, the film is also affected by the adhesion force (f_1) between the impurities on the surface and the plastic film. In the plastic-film-conveying stage, the stress of the film is the same as that of the film-hanging process.

Under the gravity of the pickup device, the nail teeth are inserted into the soil to puncture the film, and the nail teeth are unearthed under the rotation of the picking rotary drum. From the puncturing process to the picking process, the condition for the nail teeth to break the film and pick up the residual film smoothly is that the residual film does not break away from the nail teeth when the nail teeth are unearthed. From the force analysis of the residual film in the film-puncturing area, it can be seen that at point a_1, the plastic film is attached to the nail tooth and does not fall off. At this time, there is the following:

$$\begin{cases} f + F_1 \sin\alpha \geq (G_0 + G_1 + F_0)\cos\alpha \\ f = \mu F_N \\ F_N = (G_0 + G_1 + F_0)\sin\alpha + F_1 \cos\alpha \end{cases} \tag{22}$$

where μ is the friction coefficient between the residual film and the pickup nail teeth.

According to Equation (22), the weight of the impurities on the surface of the film and the adhesion between the film and the soil are uncontrollable factors. According to the structure and material of the device, the α and μ can be determined. If the nail teeth can pick up the residual film, there is the following:

$$F_1 \geq \frac{(G_0 + G_1 + F_0)(\cos\alpha - \mu\sin\alpha)}{\mu\cos\alpha + \sin\alpha} = F_2 \tag{23}$$

Among them,

$$\cos\alpha = \frac{R + h_0 + L - h}{R + h_0 + L} = 1 - \frac{h}{R + h_0 + L} \tag{24}$$

The nail teeth separate the mulching film from the soil and enter the film-picking process at this time. With the rotation of the picking rotary drum, the plastic film is deformed by the tension of the nail teeth and the gravity of the impurities on the film. The conditions for the mulching film to be picked up in the film-picking area and run smoothly to the film-hanging area are as follows: the plastic film can be attached to the nail teeth, and the tensile force is less than the breaking force of the film itself. From the residual-film stress analysis diagram, the following can be seen:

$$\begin{cases} f \geq (G_0 + G_1)\cos(\alpha + \beta) \\ f = \mu F_N \\ F_N = (G_0 + G_1)\sin(\alpha + \beta) + F_1 \end{cases} \tag{25}$$

where β is the angle between the movement of the nail teeth in the film-picking area and the unearthed nail teeth (rad).

The analysis of the plastic-film force diagram shows that the film is subjected to the maximum tension at position b. Therefore,

$$\begin{cases} F_N = G_0 + G_1 + F_1 \\ F_N \leq F_z \end{cases} \tag{26}$$

where F_z is the longitudinal maximum tensile force of the mulching film (N).

Based on the previous study [28], the longitudinal draggle force at the break of the film (F_z) with a thickness of 0.01 mm was 2.61 N, and the film mass (G_0) was ignored. Therefore,

$$G_1 + F_1 \leq 2.61 \tag{27}$$

The mass of the impurities on the film surface per unit area (1 m^2) was 10.012 kg. The impurity weight (G_1) of the film surface with a width of 140 mm and a length of 50 mm was 0.69 N. Assuming that the G_1 only acts on the plastic film with a width of 10 mm, then,

$$F_1 \leq 2.61 - G_1 = 1.92 \tag{28}$$

The degree of deformation of the film decides the value of the F_1. Based on the tensile performance test of the plastic film [28], when the tensile force of the plastic film is 1.92 N, the corresponding fracture nominal strain (ε) is 20%. Therefore, according to the definition of the nominal strain at break of the plastic film, the following can be seen:

$$\varepsilon = \frac{S - S'}{S'} \leq 20\% \tag{29}$$

where S is the length of the mulching film picked up by the pickup device at the same time (m); S' is the forward distance of the machine at the same time (m).

In the mulching-film-picking stage, the film with the picking drum performs rotary motion; thus,

$$\varepsilon = \frac{\omega_1 (R + h_0 + L)t - v_m t}{v_m t} = \frac{v_0 - v_m}{v_m} \leq 20\% \tag{30}$$

According to Equation (30) and combined with Equation (16) and the analysis in Section 2.2, the following can be obtained:

$$1 \leq \lambda = \frac{v_0}{v_m} \leq 1.2 \tag{31}$$

Bringing Equation (31) into Equation (21), it can be seen that when λ takes 1, $L_1 \leq 0.317$ m. Therefore, the maximum spacing (L_1) between two adjacent pickup nail teeth can be 285.75 mm. At this point, the tensile force received by the plastic film is less than its longitudinal breaking force, meeting the operational requirements of the picking device. The picking rotary drum performs a circular motion in the film-picking stage, and the speed of the picking rotary drum (n_1) is as follows:

$$n_1 = \frac{30 \lambda v_m}{\pi (R + h_0 + L)} \tag{32}$$

By analyzing Equations (23) and (24), it can be seen that the value of the F_2 can be reduced by reducing the trajectory radius of the pickup nail teeth. According to the forward research [20], the radius (R) of the chain-guide plate was determined to be 250 mm. The friction coefficient (μ) between the nail teeth and the film is 0.439 [29]. In clay soil, $F_0 \approx 5$ (G_0 + G_1) [30]. The weight of the impurities and residual film (G_0 + G_1) with a width of 140 mm and a length of 286 mm was 3.94 N. Then, F_0 = 19.70 N, F_2 = 3.34 N.

The maximum value of the F_1 is 2.61 N, which cannot satisfy $F_1 > F_2$. The analysis shows that due to the excessive adhesion between the residual film and the soil, the plastic film cannot be picked up after the pickup nail teeth pierce the film. Therefore, the film-lifting device is required. During the operation, the plastic film is first separated from the soil, and then it is picked up by the nail teeth to complete the plastic-film collection. In addition, field experiments showed that when there was no film-lifting device, the bonding force between the soil and the residual film was greater than the force of the pickup nail teeth on the residual film. At this time, the residual film could not be picked up. After the operation of the machine, there was a hole mark on the residual film, but the residual film was still attached to the soil [31].

In the film-hanging area, the plastic film on the nail teeth is affected by its own gravity and impurity adhesion force, and it moves from the end of the nail teeth to the root of the teeth, so that the plastic film is attached to the nail teeth more firmly and does not easily fall off. With the movement of the nail chain, the film runs to the conveying area. The impurities are separated from the film in the film-hanging and film-conveying areas.

3.5. Structure of Shovel-Type Film-Lifting Device

The film-lifting device is an essential working portion of the plastic-film-collecting machine. Its main function is to separate the residual film bonded to the surface from the soil and, at the same time, loosen the soil to avoid the difficulty of picking up the residual film due to the excessive adhesion between the film and the soil. The structure diagram of the shovel-type film-lifting device is shown in Figure 13, which is mainly composed of the film-lifting shovel, supporting circular tube, profiling connecting rod, connecting frame, depth-limiting spring, and supporting beam.

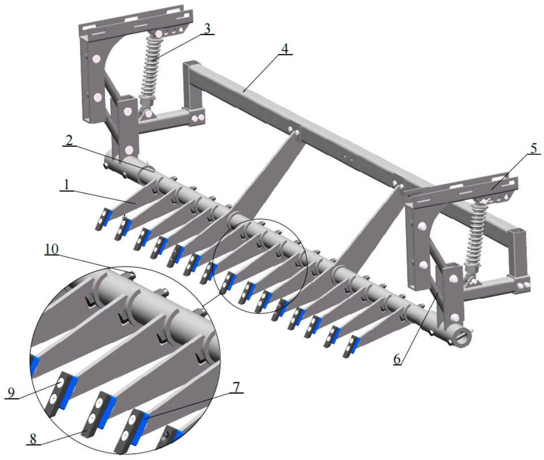

Figure 13. Structure of shovel-type film-lifting device: 1. film-lifting shovel; 2. supporting round tube; 3. depth-limiting spring; 4. supporting beam; 5. connecting frame; 6. profile connecting rod; 7. film-shovel connecting plate; 8. soil-engaging plate; 9. countersunk bolt; 10. hexagon bolt.

The shovel tip of the film shovel is designed in two parts, and the front end has a detachable soil-engaging plate. The soil-engaging plate is fixed on the main part of the shovel handle of the film shovel by the countersunk bolt. The film shovel is connected with the supporting round tube by hexagonal bolts and arranged at a certain distance. The soil-engaging plate and the film shovel are in contact with the soil and have significant wear and tear. Therefore, the design of the detachable soil-engaging plate and film shovel is convenient for replacement, saving materials and costs.

3.6. Main Parameters of Shovel Film-Lifting Device

The effect of the film-lifting operation is closely related to the layout size of the film-lifting shovels. The film shovels and the film-picking chain are staggered to ensure that when the nail teeth on each picking chain pick up the residual film, there are film shovels on both sides to provide support for the lower part of the residual film.

The more the film shovel is arranged, the larger the supporting area of the film, which is more conducive to film lifting, but it easily causes soil and straw blockage and increases the operating resistance. On the contrary, the less the film shovel is arranged, the larger the spacing, and the pressure of the impurities on the surface of the residual film is greater than the support force of the film shovel. The residual film is not easily supported by the film shovel and is dragged up and easy to miss, and this causes a low recovery rate of the residual film. According to the width of 1800~1900 mm after plastic-film mulching [32], a total of 15 film shovels were arranged on the film surface. A film shovel is arranged in the middle of two narrow rows of cotton. In order to reduce the amount of cotton stalk stubble shoveled by the film shovel, it is necessary to increase the spacing between the film shovel and the cotton stalk stubble. Therefore, the spacing of three film shovels between the cotton stalk plants was 140 mm, and the spacing of the film shovels on the wide film was 120 mm. The overall width of 15 film shovels is 1800 mm. On the basis of previous studies, it was determined that the penetration angle of the soil-engaging plate would be 60°, the width would be 25 mm, and the length would be 85 mm [32]. The main parameters of the film-lifting device are shown in Figure 14.

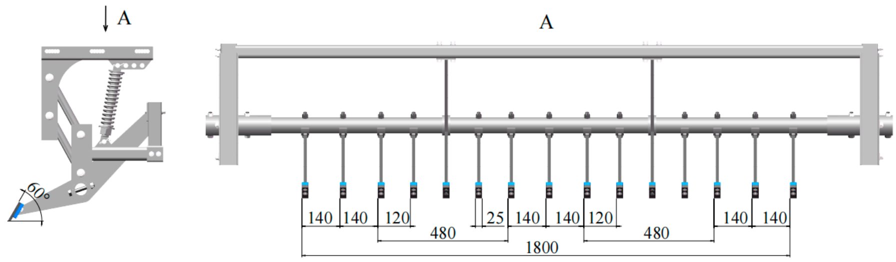

Figure 14. Schematic diagram of main parameters of film-lifting device.

3.7. Spacing and Number of Friction-Type Plastic-Film Pickup Chains

The picking effect of mulching film is closely related to the arrangement spacing of the picking chains of friction-type plastic film. The arrangement density of the plastic-film-picking chain is high, and the recovery rate of the film is high. However, impurities, including cotton shells, cotton leaves, cotton stalks, and soil blocks, are not easily separated from the residual film during the picking process, and the impurity content of the recovered residual film is high, which makes it difficult to reuse the residual film and increases the working resistance of the machine. The distance between the plastic-film-picking chains is too large, and small pieces of plastic film are difficult to pick up, which reduces the recovery rate of the film. Based on the previous test [20] and the arrangement spacing of the film shovel, the designed spacing of the film-picking chains is shown in Figure 15. A single film surface (width of 2050 mm) is arranged with 16 friction-type plastic-film-picking chains, and the arrangement spacing is shown in the figure. The size of the entire plastic-film-picking chain row is 1920 mm. Under the action of the film shovel, the residual film of a single film width can be picked up.

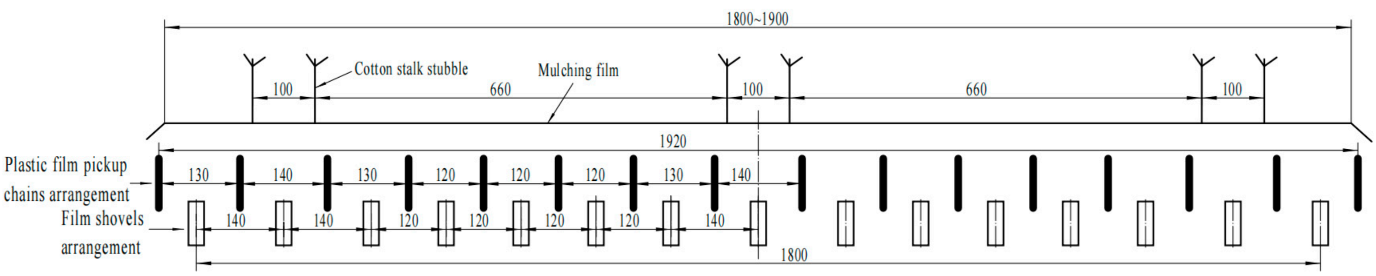

Figure 15. Distribution diagram of friction-type plastic-film pickup chains and film shovels.

4. Field Experiment

4.1. Test Conditions

According to the parameters determined in the design and an analysis of the key components of the residual-film-picking system in Section 3 and the straw-crushing device, the combined straw-crushing and residual-film-recovery machine was trial-produced. The field performance test was carried out in the 145 regiment of Shihezi City, Xinjiang, from October to November 2023, as shown in Figure 16.

(**a**) (**b**) (**c**) (**d**)

Figure 16. Field experiment: (**a**) test site conditions; (**b**) testing machine; (**c**) telemetry instrument installation; (**d**) operation process.

The thickness of the mulch film was 0.01 mm, and the drip irrigation belt had been taken out. There were many soils and impurities on the surface of the mulch film, as shown in Figure 16a. The supporting power machine was a John Deere 954 wheeled tractor, and the plastic-film-recovery machine was in good condition after debugging before the test (Figure 16b). The test was carried out according to the test method specified in the national standard GB/T 25412-2021 [33]. The test instruments mainly included electronic weighing (range: 50 kg; precision: 1 g), electronic weighing (range: 500 g; precision: 0.001 g), tape (range: 50 m; precision: 0.002 m), and an NJTY3 agricultural-machinery general dynamic telemetry instrument (Heilongjiang Academy of Agricultural Machinery Engineering Science, Harbin, Heilongjiang, China). During the test, the traction sensor of the telemetry instrument was installed between the two lower suspension points of the tractor and the traction frame of the combined-operation machine, as shown in Figure 16c. The test process is shown in Figure 16d.

4.2. Experimental Factors and Evaluation Index

To optimize the performance of the friction-type nail-tooth-chain-plate residual-film-picking system and achieve the highest operating efficiency, it was necessary to determine the optimal working parameters through experiments. From the analysis in Section 3, it can be seen that the picking-speed ratio (λ) is between 1 and 1.2. Through many experiments in the early stage, the optimal value of the pickup-speed ratio (λ) was determined to be 1.1 [21,31]. In order to improve the working efficiency, the value range of the forward speed of the machine is 4~8 km/h. According to the analysis of the plastic-film force, the maximum spacing (L_1) between the two adjacent nail teeth can be taken as 285.75 mm, and the minimum is 57.15 mm. According to the measurement results of the cotton-field surface roughness, the maximum value of the cotton-field surface roughness appears in the center of a wide row of cotton, between 25 and 45 mm [31]. In order to ensure that the film-lifting device separates the surface residual film from the soil, the depth of the film shovel into the soil is 30~50 mm. Moreover, the center distance between the shovel tip and the picking rotary drum affects the connection effect between the film lifting and the pickup. According to the soil depth of the film shovel and the contact between the nail teeth and the film shovel as the boundary conditions, the center distance between the tip of the film shovel and the picking rotary drum was determined to be 110~150 mm.

In summary, the operating speed (X_1), pickup-nail-teeth spacing (X_2), depth of the film shovel into the soil (X_3), and distance between the tip of the film shovel and the center of the picking drum (X_4) were selected as the test factors. By replacing the transmission sprocket to ensure that the pickup-speed ratio was 1.1, the operating speed was adjusted by controlling the forward speed of the tractor. Before the test, the driving speed of the tractor traction machine was tested. According to the tractor gear and engine speed, the five operating speeds of 4 km/h, 5 km/h, 6 km/h, 7 km/h, and 8 km/h, which were closest to the test requirements, were obtained through multiple tests. In the subsequent test, the tractor gear and engine speed were adjusted according to the operation speed requirements. The pickup nail teeth are detachable. By installing the pickup nail teeth at intervals on the rubber-chain friction block, the spacing of the pickup nail teeth is adjusted. The soil depth of the film shovel into the soil is changed by adjusting the depth-limiting spring of the film-lifting device, and the center distance between the tip of the film shovel and the pickup drum is changed by adjusting the position of the connecting hole between the connecting frame of the film-lifting device and the frame. A four-factor quadratic orthogonal rotation combination design was used in the experiment. The level and value of each test factor are shown in Table 1.

Table 1. Test-factor levels and coding table.

Factor Coding	Operating Speed (X_1/km·h^{-1})	Pickup-Nail-Teeth Spacing (X_2/mm)	Depth of Film Shovel into Soil (X_3/mm)	Distance between Tip of Film Shovel and Center of Picking Drum (X_4/mm)
−2	4	57.15	30	110
−1	5	114.3	35	120
0	6	171.45	40	130
1	7	228.6	45	140
2	8	285.75	50	150

The operating performance of the friction-type nail-tooth-chain-plate residual-film-picking system was evaluated by the residual-film-picking rate, the impurity rate of the recovered film, and the traction resistance, and the influence of the key parameters of the picking system on the operating performance index was obtained. After the end of each group of tests, five measuring points were selected in the test area, and each measuring point was 5 m. The unpicked plastic film on the surface within the range of the measuring point was collected, washed and dried, and weighed. The residual-film-picking rate (Y_1) was calculated according to Equation (33), and the average value was taken. At the same time, the mass of the recovered film roll and the mass of the impurities in the test area were collected, and the impurity content of the recovered residual film (Y_2) was calculated according to Equation (34). The size of the traction resistance (Y_3) was measured by an NJTY3 agricultural-machinery general dynamic telemetry instrument.

$$Y_1 = (1 - \frac{W}{W_0}) \times 100 \tag{33}$$

where Y_1 is the residual-film pickup rate (mass fraction) (%); W is the residual film that has not been picked up on the surface within the range of the measuring points after operation (g); W_0 is the residual-film mass of the ground surface before the operation (g).

$$Y_2 = \frac{W_1}{W_2} \times 100 \tag{34}$$

where Y_2 is the impurity content (mass fraction) of the recovered residual film (%); W_1 is the weight of the impurities in the recovered residual film (g); W_2 is the total weight of the recovered film roll (g).

4.3. Test Scheme and Results

According to the orthogonal test factors and horizontal coding set in Table 1, a four-factor, five-level orthogonal test was designed using the Central Composite Design (CCD) module in the experimental design and analysis software Design Expert 13, for a total of 36 groups of regression orthogonal combination tests [34,35]. The test plan and test results are shown in Table 2.

Table 2. Design scheme and results of quadratic orthogonal rotation combination test.

No.	Factors				Response Values		
	X_1	X_2	X_3	X_4	Y_1	Y_2	Y_3
1	−1	−1	−1	−1	91.92	13.13	20.528
2	1	−1	−1	−1	89.28	14.31	22.642
3	−1	1	−1	−1	87.96	11.22	19.727
4	1	1	−1	−1	88.73	10.03	19.332
5	−1	−1	1	−1	92.14	13.64	21.045
6	1	−1	1	−1	89.51	14.83	24.207
7	−1	1	1	−1	88.79	9.74	21.745
8	1	1	1	−1	89.65	10.53	21.752
9	−1	−1	−1	1	90.83	12.53	20.737
10	1	−1	−1	1	88.09	13.72	23.552
11	−1	1	−1	1	87.67	10.61	18.737
12	1	1	−1	1	87.74	8.93	19.045
13	−1	−1	1	1	88.75	12.94	22.155
14	1	−1	1	1	85.92	14.14	25.125
15	−1	1	1	1	85.68	9.04	22.252
16	1	1	1	1	86.46	10.31	20.162
17	−2	0	0	0	85.21	14.41	20.218
18	2	0	0	0	83.17	16.54	22.678
19	0	−2	0	0	87.59	15.21	23.962
20	0	2	0	0	86.17	7.51	19.332
21	0	0	−2	0	89.11	10.12	20.972
22	0	0	2	0	88.46	11.62	24.625
23	0	0	0	−2	94.12	12.33	22.482
24	0	0	0	2	86.55	9.43	22.507
25	0	0	0	0	91.35	10.14	21.375
26	0	0	0	0	92.81	9.53	20.415
27	0	0	0	0	92.54	9.64	21.280
28	0	0	0	0	91.13	10.35	21.232
29	0	0	0	0	92.57	9.54	21.357
30	0	0	0	0	91.51	10.52	20.592
31	0	0	0	0	92.66	9.83	20.565
32	0	0	0	0	93.18	9.21	20.572
33	0	0	0	0	93.39	9.39	21.182
34	0	0	0	0	92.84	9.94	21.240
35	0	0	0	0	92.62	9.54	19.822
36	0	0	0	0	93.03	10.04	21.392

4.4. Regression Model Establishment and Significance Test

The Design-Expert 13 software was used to analyze the variance in the test results, and the results are shown in Table 3. From the analysis in Table 3, it can be seen that the regression model (p) of each test index was less than 0.01, which is extremely significant. The lack-of-fit values for the residual-film pickup rate, impurity rate, and traction resistance were 2.29, 2.56, and 1.74, respectively, indicating that the lack of fit is not significant relative to the pure error. The R^2 values of the three models of the residual-film pickup rate, impurity rate, and traction resistance were 0.9340, 0.9648, and 0.9135, respectively, and the coefficients of variation ($C.V$) were 1.04%, 4.70%, and 2.76%, respectively. This shows that the three models can describe over 93%, 96%, and 91% of the response value changes, respectively. There is a high relevance between the actual value and the predicted value, and the test error is small, indicating that the regression model has a good fit with the actual situation.

Table 3. Analysis of variance of quadratic regression orthogonal rotation combination test.

Source	Y_1			Y_2			Y_3		
	Sum of Squares	F Value	p Value	Sum of Squares	F Value	p Value	Sum of Squares	F Value	p Value
Model	260.23	21.24	<0.0001 **	160.68	41.11	<0.0001 **	77.19	15.83	<0.0001 **
X_1	6.45	7.37	0.013 *	2.81	10.06	0.0046 *	7.95	22.82	0.0001 **
X_2	11.48	13.12	0.0016 **	81.51	292.01	<0.0001 **	29.26	84.02	<0.0001 **
X_3	1.83	2.09	0.1634	0.5673	2.03	0.1687	19.17	55.05	<0.0001 **
X_4	42.61	48.68	<0.0001 **	5.05	18.09	0.0004 **	0.0292	0.0838	0.775
X_1X_2	11.09	12.67	0.0019 **	1.94	6.95	0.0155 *	10.94	31.42	<0.0001 **
X_1X_3	0.0324	0.037	0.8493	1.53	5.49	0.0291 *	0.0393	0.1129	0.7402
X_1X_4	0.0729	0.0833	0.7757	6.25×10^{-6}	0	0.9963	0.049	0.1406	0.7115
X_2X_3	0.3249	0.3712	0.5489	0.5738	2.06	0.1664	0.9985	2.87	0.1052
X_2X_4	0.1764	0.2015	0.6581	0.0002	0.0006	0.9813	1.9	5.44	0.0297 *
X_3X_4	5.9	6.75	0.0168 *	0.0218	0.0779	0.7828	0.076	0.2183	0.6451
${X_1}^2$	112.93	129.01	<0.0001 **	59.92	214.67	<0.0001 **	0.0125	0.0358	0.8517
${X_2}^2$	46.55	53.18	<0.0001 **	3.69	13.23	0.0015 **	0.1545	0.4437	0.5126
${X_3}^2$	17.04	19.47	0.0002 **	1.51	5.41	0.0302 *	4.09	11.74	0.0025 **
${X_4}^2$	3.75	4.28	0.051	1.54	5.53	0.0285 *	2.53	7.27	0.0135 *
Residual	18.38			5.86			7.31		
Lack of Fit	12.42	2.29	0.0949	4.1	2.56	0.0698	4.48	1.74	0.1888
Pure Error	5.96			1.76			2.83		
Cor Total	278.61			166.54			84.5		
R^2		0.9340			0.9648			0.9135	
R^2_{adj}		0.8900			0.9413			0.8558	
$C.V$		1.04			4.70			2.76	

** $p < 0.01$, very significant; * $0.01 \le p < 0.05$, significant.

From the p value in the variance analysis results, it can be seen that the pickup-nail-teeth spacing (X_2) and the distance between the film-shovel tip and the pickup drum center (X_4) had a very significant impact on the residual-film pickup rate (Y_1), and the operating speed (X_1) had a significant impact on the Y_1. The interaction terms X_1X_2 and X_3X_4 were extremely significant or significant influencing factors of the test evaluation index Y_1. The test factors X_1, X_2, and X_4 had a significant effect on the impurity rate of the residual film (Y_2). The interaction terms X_1X_2 and X_1X_3 were the significant influencing factors of the test evaluation index Y_2. The influence of the test factors X_1, X_2, and X_3 on the traction resistance (Y_3) was very significant. The interaction terms X_1X_2 and X_2X_4 were extremely significant or significant influencing factors of the test evaluation index Y_3. The regression equations of the residual-film pickup rate (Y_1), impurity rate (Y_2), and traction resistance (Y_3) were established as follows:

$$\begin{aligned} Y_1 = {} & 92.47 - 0.5183X_1 - 0.6917X_2 - 0.2758X_3 - 1.33X_4 + 0.8325X_1X_2 + 0.045X_1X_3 - 0.0675X_1X_4 \\ & + 0.1425X_2X_3 + 0.105X_2X_4 - 0.6075X_3X_4 - 1.88{X_1}^2 - 1.21{X_2}^2 - 0.7298{X_3}^2 - 0.3423{X_4}^2 \end{aligned} \tag{35}$$

$$Y_2 = 9.81 + 0.3421X_1 - 1.84X_2 + 0.15375X_3 - 0.4588X_4 - 0.3481X_1X_2 + 0.3094X_1X_3 + 0.0006X_1X_4 \\ -0.1894X_2X_3 - 0.00312X_2X_4 + 0.0369X_3X_4 + 1.37X_1{}^2 + 0.3397X_2{}^2 + 0.2172X_3{}^2 + 0.2197X_4{}^2 \tag{36}$$

$$Y_3 = 20.92 + 0.5755X_1 - 1.1X_2 + 0.8937X_3 + 0.0349X_4 - 0.8269X_1X_2 - 0.0496X_1X_3 - 0.0553X_1X_4 \\ +0.2498X_2X_3 - 0.3442X_2X_4 + 0.0689X_3X_4 + 0.0197X_1{}^2 + 0.0695X_2{}^2 + 0.3574X_3{}^2 + 0.2814X_4{}^2 \tag{37}$$

4.5. Operation Parameter Optimization and Experimental Verification

In order to make the friction-type nail-tooth-chain-plate residual-film-picking system work best, it is necessary that the picking system has a good film-picking effect, clean separation of the residual film and impurities, and low traction resistance. Because the influence of each test factor on the test index is inconsistent, it is necessary to carry out global multi-objective optimization. Taking the pickup rate of the residual film, the impurity rate of the recycled residual film, and the traction resistance as the objective functions, the four experimental factors of the pickup system, the operating speed, spacing of the nail teeth, depth of the film-lifting shovel into the soil, and center distance between the film shovel tip and pickup drum, were optimized and solved, and the constraint conditions were set, as shown in Equation (38):

$$\begin{cases} \max Y_1(X_1, X_2, X_3, X_4) \\ \min Y_2(X_1, X_2, X_3, X_4) \\ \min Y_3(X_1, X_2, X_3, X_4) \\ 4 \leq X_1 \leq 8 \\ 57.15 \leq X_2 \leq 285.75 \\ 30 \leq X_3 \leq 50 \\ 110 \leq X_4 \leq 150 \end{cases} \tag{38}$$

The optimal parameters obtained by solving in Design-Expert 13 software were as follows. With an operating speed of 6.06 km/h, a picking-nail-tooth spacing of 219.78 mm, film-shovel depth of 37.07 mm, and film-shovel-tip and picking-drum-center distance of 129.94 mm, the pickup rate of residual film (Y_1) is 90.87%, the impurity rate of recycled residual film (Y_2) is 8.57%, and the traction resistance (Y_3) is 19.505 kN. In order to verify the reliability of the model prediction results, it was necessary to verify the optimal parameters in the prototype test. Considering the feasibility of the test, the operating speed was set to 6 km/h, the spacing between the picking nail teeth was set to 228.6 mm, the depth of the film shovel into the soil was 37 mm, and the distance between the tip of the film shovel and the center of the picking drum was 130 mm. Three repeated tests were carried out under the optimized conditions, and the average value of the test results was taken.

The test shows that, under the optimal parameter combination, the average picking rate of mulching film is 90.12%, the average impurity rate of recycled residual film is 8.96%, and the average traction resistance is 19.905 kN. Through experimental analysis, it can be seen that the relative error between the experimental value and optimized value of the residual-film pickup rate is 0.83%, the relative error of the impurity rate of the recovered residual film is 4.55%, and the relative error of the traction resistance is 2.05%. The test results are close to the predicted values of the model, indicating that the parameter optimization model is accurate and reliable.

5. Conclusions

(1) In this study, a friction-type nail-tooth-chain-plate film-picking system was designed, which is mainly composed of a friction-type film-picking chain and shovel-type film-lifting device. The friction-type film-picking chain can not only avoid overload and slip during operation but also facilitates the installation of functional components to pick up the nail teeth. The shovel-type film-lifting device separates the surface residual film from the soil and assists in the film picking;

(2) The working mechanism, movement, and residual-film force of the friction-type plastic-film-picking chain were analyzed, and the conditions for realizing residual-

film picking, no-leakage picking, and conveying were determined. At the same time, the key parameters of the friction-type plastic-film-picking chain and the film-lifting device were determined;

(3) A four-factor and five-level quadratic regression orthogonal combination test was carried out with the operating speed, spacing of the pickup nail teeth, depth of the film shovel into the soil, and distance between the tip of the film shovel and the center of the picking drum used as the test factors, and the residual-film-picking rate, impurity rate, and traction resistance used as the test indexes. The influence of each test factor on the test index of the residual-film-picking system was analyzed, and the regression model was established. The optimal parameter combination was obtained by the multi-objective optimization method;

(4) Test verification shows that when the working speed is 6 km/h, the spacing of the pickup nail teeth is 228.6 mm, the depth of the film shovel is 37 mm, and the center distance between the tip of the film shovel and the pickup drum is 130 mm, the residual-film pickup rate is 90.12%, the impurity rate of the recovered residual film is 8.96%, and the traction resistance is 19.905 kN. The relative error between the experimental results and the predicted values of the regression model is less than 5%, indicating that the parameter optimization regression model is reliable, and the designed friction-type nail-tooth-chain-plate plastic-film-picking system meets the technical requirements of residual-film recovery. The research results can provide a technical reference for the research and development of residual-film-recycling machines.

Author Contributions: Conceptualization, D.J.; methodology, D.J. and J.Z.; software, T.W. and X.F.; validation, L.Y.; data curation, J.Z. and T.W.; writing—original draft preparation, D.J.; writing—review and editing, X.C. and L.Y.; supervision, X.C.; funding acquisition, L.Y. All authors have read and agreed to the published version of the manuscript.

Funding: This research was funded by the Science and Technology Department of Xinjiang Uygur Autonomous Region (grant number 2022B02020-4), the National Key Research and Development Program of China (grant number 2022YFD2002403), the Financial Science and Technology Plan Project of Xinjiang Production and Construction Corps (2023AB014), and the China Agriculture Research System—Cotton (grant number CARS-15-23).

Institutional Review Board Statement: Not applicable.

Data Availability Statement: All data are presented in this article in the form of figures and tables.

Conflicts of Interest: The authors declare no conflicts of interest.

References

1. Steinmetz, Z.; Wollmann, C.; Schaefer, M.; Buchmann, C.; David, J.; Tröger, J.; Munoz, K.; Frör, O.; Schaumann, G.E. Plastic mulching in agriculture. Trading short-term agronomic benefits for long-term soil degradation? *Sci. Total Environ.* **2016**, *550*, 690–705. [CrossRef] [PubMed]
2. Zhao, Y.; Li, G.A.; Xia, J.B.; Bo, L.Y.; Mao, X.M. Effects of film mulching and irrigation amount on the root distribution and yield of seed-maize. *Trans. Chin. Soc. Agric. Eng.* **2022**, *38*, 104–114. [CrossRef]
3. Wang, H.J.; Wang, M.; Wang, J.L.; Lu, Y.T.; Ying, Y.K.; He, Y.Z. Control technology and control strategy of residual film pollution in Xinjiang farmland. *J. Chin. Agric. Mech.* **2022**, *43*, 166–174. [CrossRef]
4. Liu, J.G.; Li, Y.B.; Zhang, W.; Sun, Y.Y. The Distributing of the residue film and influence on cotton growth under continuous cropping in oasis of Xinjiang. *J. Agro-Environ. Sci.* **2010**, *29*, 246–250.
5. Fu, L.H.; Ye, L.Q. *China Statistical Yearbook*; China Statistics Press: Beijing, China, 2023. Available online: https://www.stats.gov.cn/sj/ndsj/2023/indexch.htm (accessed on 15 January 2024).
6. Yang, J.K.; Zhai, Z.Q.; Li, Y.L.; Duan, H.W.; Cai, F.J.; Lv, J.D.; Zhang, R.Y. Design and research of residual film pollution monitoring system based on UAV. *Comput. Electron. Agric.* **2024**, *217*, 108608. [CrossRef]
7. Rochman, C.M. Microplastics research—From sink to source. *Science* **2018**, *360*, 28–29. [CrossRef]
8. Jin, W.; Liu, J.Y.; Xu, C.B.; Zhang, X.J.; Bai, S.H. Design, simulation and experimentation of a polythene film debris recovery machine in soil. *Appl. Sci.* **2022**, *12*, 1366. [CrossRef]
9. Xie, J.H.; Zhang, Y.H.; Cao, S.L.; Zhang, Y.; Zhou, J.B.; Meng, Q.H. Design and experiment of stalk pressing type cotton field mulch film collectors. *Trans. Chin. Soc. Agric. Eng.* **2023**, *39*, 51–63. [CrossRef]

10. Peng, Q.J.; Li, K.K.; Wang, X.Y.; Zhang, G.H.; Kang, J.M. Design and test of stripping and impurity removal device for spring-tooth residual plastic film collector. *Agriculture* **2023**, *13*, 42. [CrossRef]
11. Wang, F.; Dai, F.; Zhang, F.W.; Song, X.F.; Shi, R.J.; Zhao, W.Y.; Ma, H.J. Simulation analysis and test on the effect of picking up the residual film of typical film lifting parts. *Agronomy* **2023**, *13*, 488. [CrossRef]
12. Liu, J.B.; Zheng, X.; Zhao, Y.; Liu, X.A.; Ge, S.L. Design and experiment of a new rod-tooth-roller′ plastic film residue collector. *Agric. Res. Arid Areas* **2017**, *35*, 300–306. [CrossRef]
13. Liu, X.L.; Zhao, W.Y.; Zhang, H.; Wang, G.P.; Sun, W.; Dai, F.; Li, H.; Xin, S.L. Design and experiment of an upper-side-discharge straw-returning and bundle self-unloading integrated corn residual film recycling machine. *Int. J. Agric. Biol. Eng.* **2023**, *16*, 61–70. [CrossRef]
14. Cao, S.L.; Xie, J.H.; Wang, H.Z.; Yang, Y.X.; Zhang, Y.H.; Zhou, J.B.; Wu, S.H. Design and operating parameters optimization of the hook-and-tooth chain rail type residual film picking device. *Agriculture* **2022**, *12*, 1717. [CrossRef]
15. Dong, J.H.; Wang, J.; Bi, X.S.; Zheng, Y.J.; Wang, G.H.; Wang, J.K.; Chen, Y.; Jia, J. Analysis and test of clamp conveying type residual film recycling and film impurity separation mechanism. *Processes* **2022**, *10*, 1816. [CrossRef]
16. Kou, J.L.; Wang, J.K.; Wang, L.; Zhao, Y.M. Integrating clamping finger-chain residual film recycling and straw crushing return to cotton field. *Trans. Chin. Soc. Agric. Eng.* **2023**, *39*, 14–22. [CrossRef]
17. Cao, S.L.; Xie, J.H.; Yang, Y.X.; Liu, Y.R.; Lu, Y.T.; Sun, B. Design and experiment of side row cotton straw returning and residual film recovery combined machine. *J. Jilin Univ. Eng. Technol. Ed.* **2023**, *53*, 1514–1528. [CrossRef]
18. Xie, J.H.; Yang, Y.X.; Cao, S.L.; Zhang, Y.; Zhou, Y.B.; Ma, W.B. Design and experiments of rake type surface residual film recycling machine with guide chain. *Trans. Chin. Soc. Agric. Eng.* **2020**, *36*, 76–86. [CrossRef]
19. Shi, Z.L.; Zhang, X.J.; Cheng, J.P.; Zhou, X.C.; Zhang, C.S. Design and test of film transfer and unloading device of vertical double-row chain residual film recycling machine. *Agric. Res. Arid Areas* **2023**, *41*, 257–265.
20. Yang, S.M.; Yan, L.M.; Mo, Y.S.; Chen, X.G.; Zhang, H.M.; Jiang, D.L. Design and experiment on collecting device for profile modeling residual plastic film collector. *Trans. Chin. Soc. Agric. Mach.* **2018**, *49*, 109–115, 164. [CrossRef]
21. Jiang, D.L.; Chen, X.G.; Yan, L.M.; Mo, Y.S.; Yang, S.M.; Wang, Z.Y. Optimization of working parameters of cleaning system for master-slave residual plastic film recovery machine. *Trans. Chin. Soc. Agric. Eng.* **2019**, *35*, 1–10. [CrossRef]
22. Wang, D.W.; Wang, Z.H.; Zhang, J.Z.; Lv, T.B.; Zhou, B.; Li, W.H. Effects of drip tape modes on machine-harvest cotton growth and soil water, heat and salt distribution in Northern Xinjiang of China. *Trans. Chin. Soc. Agric. Eng.* **2022**, *38*, 76–86. [CrossRef]
23. Wang, M.M.; Lv, T.B.; He, X.L.; Cao, Y.B.; Wang, D.W. Effects of drip-irrigated planting modes on soil water, temperature, salt and cotton growth. *Agric. Res. Arid. Areas* **2018**, *36*, 176–186.
24. Creery, L.C. Speed and Load Estimation of Chain Drive Using Extended Kalman Filter and Artificial Neural Networks. Master's Thesis, University of Arizona, Tucson, AZ, USA, 2023.
25. Chen, X.B.; Zhang, H.; Liu, Y.; Wang, J.Y.; Song, J.Q. Influence on polygon effect with characteristic parameters of guide arc branch of the crawler robot. *Int. J. Heavy Veh. Syst.* **2024**, *31*, 32–48. [CrossRef]
26. Pu, L.G.; Chen, G.D.; Wu, L.Y. *Mechanical Design*; Higher Education Press: Beijing, China, 2019; p. 156.
27. Liu, C.; Hu, B.; Luo, X.; Guo, M.Y.; Li, Z.Y.; He, Z.X.; Chen, Z.L.; Xie, Y.Y. Design and test of residual film recovery machine based on drum elastic tooth film lifting mechanism. *J. Gansu Agric. Univ.* **2022**, *57*, 230–239. [CrossRef]
28. Jiang, D.L.; Chen, X.G.; Yan, L.M.; Yang, J.C.; Li, Y. Mechanical and friction properties of agricultural plastic film during autumn harvest period of cotton in Xinjiang, China. *Environ. Sci. Pollut. Res.* **2023**, *30*, 89238–89252. [CrossRef] [PubMed]
29. Liang, R.Q. Study on the Cutting Characteristics of Residual Film and Impurities for Machine Harvesting in Cotton Field with Multi-Edge Tooth Cutter. Doctoral Dissertation, Shihezi University, Shihezi, China, 2022.
30. Xu, H.B.; Hu, Z.C.; Wu, F.; Gu, F.W.; Yu, Z.Y. Contrastive analysis and experiment of conveying mode for chain-tooth plastic film residue collector. *J. Agric. Mech. Res.* **2017**, *5*, 12–20.
31. Yang, S.M. Design and Key Technology Research of Passive Cotton Field Residual Plastic Film Recycling Machine. Doctoral Dissertation, Jilin University, Changchun, China, 2020.
32. Yang, S.M.; Chen, X.G.; Yan, L.M.; Jiang, D.L. Performance of three different spades for residual plastic film recycling machine. *Appl. Eng. Agric.* **2020**, *36*, 187–195. [CrossRef]
33. *GB/T 25412-2021*; Farm Waste Film-Pick Up Machines. Standards Press of China: Beijing, China, 2021.
34. Lin, J.; Zhang, T.J.; Tian, Y.; Gao, W.Y.; Qi, L.; Li, B.F. Optimization and experiment on bionic deep-buried device for returning straw in field. *Trans. Chin. Soc. Agric. Mach.* **2018**, *49*, 50–59, 67. [CrossRef]
35. Fang, F.; Xu, K.Y.; Luo, Z.Y.; Chen, Y. Optimization of aqueous enzymatic extraction of kiwi-fruit seed oil by quadratic regression orthogonal design. *J. Chin. Cereals Oils Assoc.* **2013**, *28*, 55–59. [CrossRef]